Nonuniform Absorption and Scattered Light in Direct-Drive Implosions Driven by Polarization Smoothing

D. H. Edgell, P. B. Radha, J. Katz, A. Shvydky, D. Turnbull⬤, and D. H. Froula

Laboratory for Laser Energetics, University of Rochester, 250 East River Road, Rochester, New York 14623-1299, USA

Laser-direct-drive symmetric implosions on OMEGA illuminate a target with 60 laser beams and are designed to produce spherical implosions. Each beam is smoothed using orthogonal polarizations obtained by passing the laser beams through distributed polarization rotators (DPRs). Observations of light scattered from OMEGA implosions do not show the expected symmetry and have much larger variation than standard predictions. For the first time, we have quantified the scattered-light nonuniformity from individual beams and identified the DPRs as the source of the enhanced nonuniformity. An instrument was invented that isolated and measured the variation in the intensity and polarization of the light scattered from each OMEGA beam. The asymmetric intensity and polarization measurements are explained when the on-target offsets between the two orthogonal polarizations produced by the DPRs are modeled using a 3D cross-beam energy transfer (CBET) code that tracks the polarizations of each beam. The time-integrated nonuniformity in laser absorption and scattered light due to CBET and the DPR polarization offsets during high-performance OMEGA implosions is predicted to be significant and dominated by low spherical harmonic mode numbers. The nonuniformity is predicted to be greatly reduced by replacing the DPRs with new optics that create smaller offsets.

The laser-direct-drive ignition [1] approach to inertial confinement fusion uses multiple symmetrically distributed lasers to illuminate a spherical capsule containing thermo-nuclear fuel (deuterium-tritium). The laser energy is deposited in a coronal plasma primarily by inverse bremsstrahlung absorption, where it is transported to an ablation surface deeper in the plasma by electron thermal conduction. Expansion of the ablated material drives the implosion and compresses the target shell and fuel to fusion pressures and temperatures. To minimize low-mode nonuniformities and hydrodynamic instabilities that quench the implosion, the compression is required to be symmetric [2,3]. Simulations suggest that the laser-irradiation nonuniformity must be below the 1% rms level to achieve ignition [3]. Projections of the laser beam intensity profiles on a sphere with a typical radius of 860 μm predict that the laser energy absorption will be very uniform (0.1% rms) over the target [4].

Simulations of direct-drive implosions suggest that cross-beam energy transfer (CBET) [5,6] redistributes the energy deposition, reducing the overall absorption efficiency [7]. The CBET process is similar to stimulated Brillouin scattering, where the ponderomotive force of the electron electromagnetic beat wave between crossing laser beams in a plasma drives a density oscillation that transfers energy from the higher-frequency beam to the lower-frequency beam. The magnitude of the ponderomotive potential $|\tilde{\varphi}|$ driving the interaction is proportional to the projection of the laser beams' electromagnetic-field polarization directions $\hat{x}_m$ and $\hat{x}_n$ onto each other [8,9]:

$$|\tilde{\varphi}| = \frac{1}{2}\frac{e}{r_e}|\tilde{a}_m||\tilde{a}_n|(\hat{x}_m \cdot \hat{x}_n),$$

where r_e is the classical electron radius, $a = (1/2)\tilde{a}\exp(i\psi)\hat{x} + \text{c.c.}$ is the vector potential of the linearly polarized beams, ψ is the phase of the beam, and $\hat{x}$ is the unit vector in the direction of its polarization. Historically, hydrodynamic codes with CBET to models for direct-drive implosions assume that the polarizations are well mixed and uncorrelated by polarization smoothing such that $(\hat{x}_m \cdot \hat{x}_n)$ can be replaced by the ensemble averaged factor $(1/2)\sqrt{1 + \cos^2(\theta)}$ (Ref. [8]). These simulations show an increased variation of absorption over the target [10], but experimental measurements of the associated scattered light assume uniform 4π scattering in order to infer the absorbed energy [11].

In this Letter, the first nonuniform scattered-light measurements are presented that reveal a novel issue that introduces significant on-target intensity modulations in direct-drive implosions through the effects of polarization on CBET. An instrument was invented that simultaneously measures the scattered light exiting the coronal plasma from all on-target laser beams. These measurements show significant beam-to-beam variation in scattered light for beams with identical deflection geometries into the
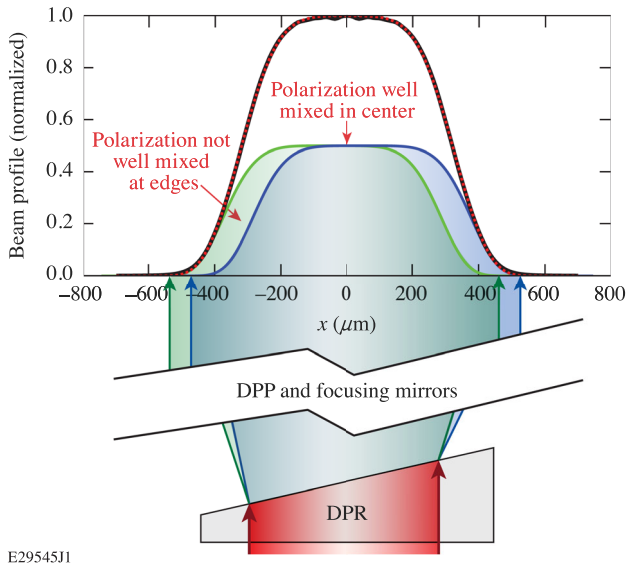
FIG. 1. The DPRs equally split each initial beam into two subbeams with equal intensity but orthogonal polarizations (green and blue curves). A small difference in direction between the two subbeams results in a significant offset in their overlap at the target (red curve) and a nonuniform polarization composition across this target beam profile.

diagnostic. A 3D CBET model was developed to follow the evolution of the polarization of each beam as it propagates through the plasma and interacts with crossing beams. The simulations show that the measured beam-to-beam variation in scattered light is a result of the sensitivity of CBET to the polarization of crossing beams. The polarization scheme on OMEGA creates regions of linear polarization at the edges of the incident laser beams, which, in turn, creates regions of preferential CBET generation determined by the specific polarization orientations of the beams as they cross through one another. This nonuniform scattering was shown to produce significant absorption nonuniformities (5.4% peak to valley) along with an underlying low mode, both driving the capsule uniformity beyond the 1% rms requirement for hydrodynamic-equivalent ignition conditions on OMEGA.

The experiments were performed on laser-direct-drive implosions using the 60-beam OMEGA laser [12]. The implosion used a 21.6-kJ square laser pulse with a room temperature plastic target (see Supplemental Material [13] for details). Distributed polarization rotators (DPRs) [14] were deployed on each OMEGA beam to split the initially linearly polarized beams into two equal-intensity beams with orthogonal polarizations (Fig. 1). The two split beams exit the DPR with a minute difference in direction ($\sim$47 μrad). After the beams were focused onto the target, this small angular difference resulted in an offset of 90 μm between the two split beams. Prior to the focus lens, each beam propagated through a distributed phase plate (DPP), which determined the super-Gaussian ($m \sim 5$, FWHM

$\sim$860-μm) intensity profile on target. The offset between the orthogonally polarized beams produced a total overlapped beam profile on the target where the two orthogonal polarizations were evenly mixed at its center. In the direction of the offset, there were two opposite regions of mostly linearly polarized light in the far-field beam profile (Fig. 1). The DPR beam split was designed to reduce the high-mode, on-target nonuniformity from laser speckles by a factor of $\sqrt{2}$, and DPR deployment is standard on high-performance implosions on OMEGA; however, as we show below, these regions of linearly polarized light are the source of low-mode asymmetry that has gone unidentified until now.

The 3ω gated optical imager (3ωGOI) scattered-light diagnostic [15,16] was developed to diagnose the nonuniformity of the light scattered from an implosion. It simultaneously collects scattered light from each of the 60 OMEGA laser beams (Fig. 2). With an image plane at the center of the target, the scattered light appears as a symmetric pattern of 60 distinct spots, each beamlet corresponding to light collected from one of the 60 beams. This beamlet is a small component of the light originating from a specific point in the far-field spatial profile of the beam and following a path through the plasma determined by refraction [Fig. 2(a)]. The intensity of the beamlet varies along its path due to absorption and CBET until it exits the plasma and ultimately reaches its end point at the diagnostic collection optic. An important feature of the 3ωGOI is its Wollaston prism that splits the collected light into orthogonal horizontal and vertical polarization components that are imaged simultaneously [Fig. 2(b)]. This diagnostic polarization split of the collected light at the diagnostic port is not correlated with the DPR polarization splits of the individual lasers but can be used to diagnose them. The beamlets are analyzed using image registration to align the two polarization subimages to a common coordinate system and identifying a region of interest (ROI) that isolates each individual beamlet spot. The sum of the pixel counts inside each ROI provides the relative intensity of a beamlet in the horizontal and vertical polarization subimages, H_b and V_b, respectively. The beamlet polarizations and total relative intensities are given by $P_b = \tan^{-1}(H_b/V_b)$ and $I_b = H_b + V_b$, respectively. More details on the 3ωGOI design and images can be found in Ref. [15], while specifics on the analysis of the beamlets in the images are detailed in Ref. [16].

The 3ωGOI was used to study the nonuniformity of the scattered light by examining the intensity of the beamlet spots in its images. In a symmetric implosion, all beamlets collected from beams at the same angular distance to the diagnostic are imaged at the same radial distance from the center of the spot pattern. Each beamlet in such a group has traveled along equivalent paths due to the beam symmetry and diagnostic geometry. If all beams were evenly split by polarization smoothing into two orthogonal polarizations
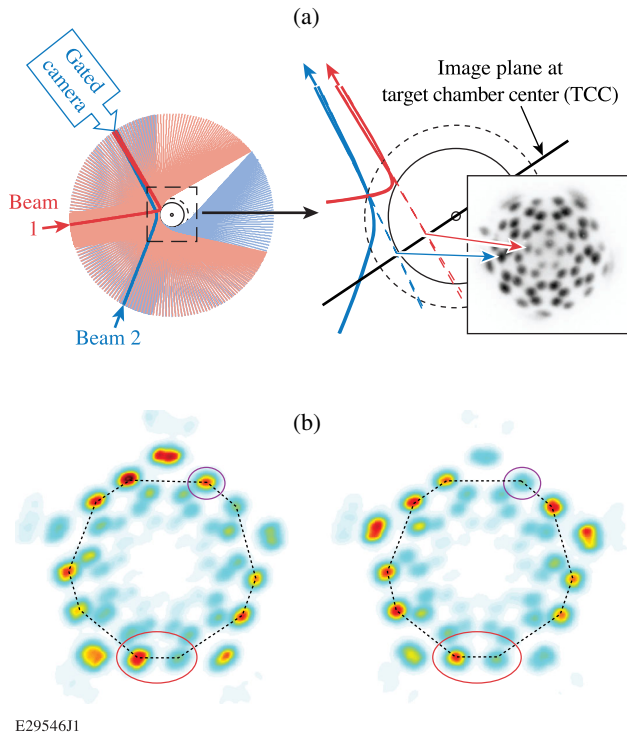
(a)

(b)

E29546J1

FIG. 2. (a) The gated optical imager collects a beamlet of scattered light from each beam that, when imaged at the target plane, appears as a distinct spot. The image on the left shows many ray paths from two color-coded beams (red and blue) refracting through the coronal plasma before exiting with diverging paths out to the chamber wall. The two bold paths (one red, one blue) illustrate the single beamlet from each beam that is collected by the 3ωGOI. The image on the right shows the 3ωGOI focal plane at target chamber center. The projection of each diverging beamlet incident on the detector is a localized spot in the focal plane. (b) The 3ωGOI uses a Wollaston prism to separate the collected light by its polarization into two separate beamlet subimages (vertical polarization on the left and horizontal on the right). The image shown here was collected near the end of a 1-ns square pulse, room temperature implosion when CBET was predicted to be strong (more details are given in Supplemental Material [13]). The dotted lines intersect the beamlets from a group of beams with the same required deflection angle to reach the diagnostic. In a symmetric implosion, all the beamlets from this beam group would have the same total intensity when the two polarization images are added together, but one can clearly see that the two beamlets highlighted by the red oval in each subimage have significantly different intensities. Furthermore, the magenta circles highlight the fact that the observed beamlet intensity can vary in each polarization subimage, indicating that the collected scattered light is polarized.

throughout their far-field profiles, then each beamlet in the group would experience the same CBET and absorption along their paths and would have similar total beamlet intensities measured by the 3ωGOI. As highlighted by the red ovals in Fig. 2(b), the measured intensities of beamlets in the same group are significantly different, indicating that
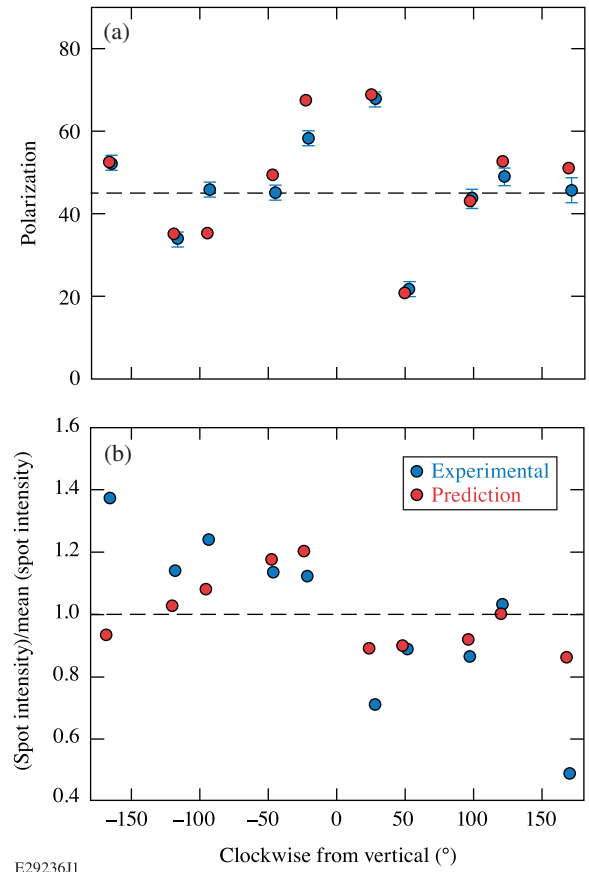

E29236J1

FIG. 3. Measured (blue circles) and predicted (red circles) values for the beamlet (a) polarization and (b) intensity as a function of the angle from vertical are plotted for the beam group identified by the dotted line in Fig. 2.

the scattered light is very asymmetric. The significant differences in the beamlet intensities between the two polarization images also show that the scattered light is strongly polarized despite the DPRs initially evenly splitting the beams into two equal orthogonal polarizations.

Figure 3 shows the observed variation (blue circles) in beamlet polarization and total relative intensity for the set of beamlets in the radial group outlined by the dotted line in Fig. 2 measured during the implosion. Truly symmetric laser absorption and CBET would have produced constant relative intensity [the dotted line in Fig. 3(b)]. Without CBET, the measured beamlet polarizations would all be at 45° [the dotted line in Fig. 3(a)] given the equal initial orthogonal polarizations introduced in each beam by the DPRs. Energy exchange due to CBET can rotate the polarization components in the beams [9], but in a symmetric implosion the polarization would be altered identically for each beam and the beamlet polarizations recorded by the 3ωGOI would show symmetry about the vertical and horizontal axes due to the Wollaston prism orientation. No such symmetry about these axes (0°/180° and +90°/−90°, respectively) is observed in Fig. 3(a). Both the observed intensity and polarization of the

beamlets indicate that the scattered light from an OMEGA implosion is highly asymmetric.

To understand the source of the observed asymmetry, absorption and scattering for all 60 OMEGA beams were modeled using a 3D CBET code [10]. This code models each OMEGA beam as a bundle of many individual beamlets propagating through plasma profiles produced by the 1D hydrodynamics code LILAC [11,17], which included a 1D CBET model [18]. Along each beamlet path, the crossings with all other beams were determined, and the 3D CBET code follows the effects of absorption and CBET for each beam, including the polarization rotation due to CBET [9]. Beamlet spot images for the 3ωGOI diagnostic are synthesized using the intensity, polarization, and propagation direction of the beamlets exiting the plasma. More details on the 3D CBET code can be found in Ref. [10] and in Supplemental Material [13].

The DPR polarization split was modeled in the code by treating each beam as a pair of independent copropagating beams with orthogonal linear polarizations, where the orientations and offsets were specified by the OMEGA system geometry. When both the DPR-produced polarizations and offsets were used to predict the beamlet polarizations and intensities (red circles in Fig. 3), the measured variation in both is explained. The high correlation between the measured and predicted polarization of the beamlets in Fig. 3(a) demonstrates the accuracy of the modeling, while the correlation between the measured and predicted intensity of the beamlets provides confirmation that the DPRs are responsible for the observed asymmetry in the scattered light. Note that, while most beamlet intensities are well matched by the modeling, a couple are not even though their polarization is. This discrepancy is not due to beam power imbalance, because the measured beam powers were used in the simulations, and the OMEGA beam power variation was too small (2.2% rms) to have a significant effect. Possible explanations for this remaining discrepancy include the beam mispointing, differences in the individual beam intensity profiles, and 3D perturbations in the coronal density profile. These possibilities are discussed in Supplemental Material [13]. Since the measured beamlet spot intensities show even greater variation than the predictions, this may suggest that the global asymmetries in absorption and scattered light over an implosion discussed below could be worse than the current predictions, depending on the source of the discrepancy.

The DPR offsets in the OMEGA beams have no symmetry in their orientation directions when the beams reach the target chamber, so enhanced CBET in the strongly polarized regions created by the DPR split offset is a source of asymmetry during an implosion. To illustrate the magnitude of this effect can have on high-performance implosions relevant to inertial confinement fusion research, the 3D CBET model was applied to a typical OMEGA cryogenic target implosion (details on the implosion are

(a) I_{out} (J/sr) = 731.3±5.42% rms   (b) I_{abs} (J/sr) = 1487.2±0.84% rms

−10   0   10
Difference from mean (%)

−2   −1   0   1   2
Difference from mean (%)

(c) I_{out} (J/sr) = 653.8±0.92% rms   (d) I_{abs} (J/sr) = 1505.5±0.44% rms
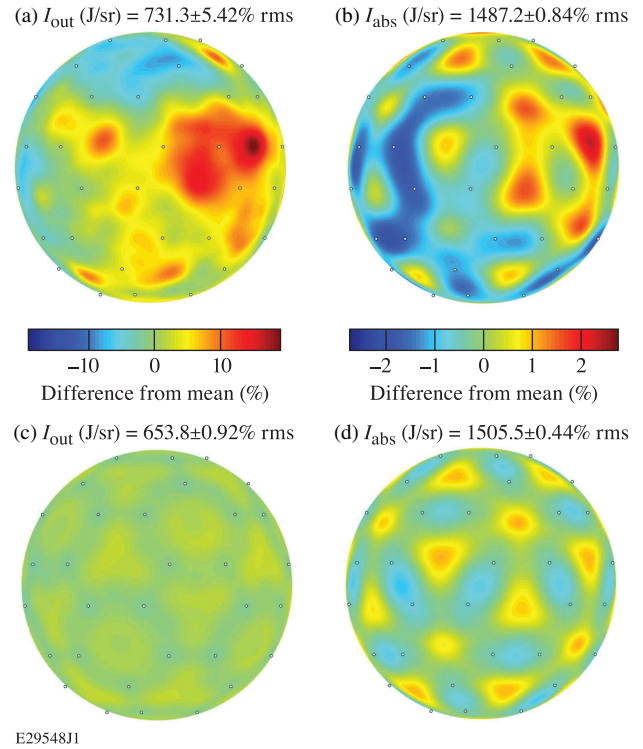

E29548J1

FIG. 4. Predicted variation from mean of the (a) scattered light and (b) absorption radiant exposure (J/sr) distributions over a spherical surface for an OMEGA cryogenic implosion using the current DPRs that create a 90-μm offset on target chamber center between the polarization split subbeams. If new DPRs that create an offset of only 10 μm are fabricated and deployed on OMEGA, the predicted variation from mean distributions for (c) scattered light and (d) absorption show a greatly improved uniformity.

given in Supplemental Material [13]). Using the DPR + CBET modeling, the total time-integrated nonuniformity was calculated. Beam power imbalance and beam mispointing were not included in this modeling to isolate the DPR-induced effect. Figures 4(a) and 4(b) show that the total time-integrated nonuniformity over the entire course of an implosion due to CBET and the DPR-polarization split was predicted to be significant for an otherwise symmetric implosion. Figure 4(a) shows the calculated total scattered light over the inner surface of the target chamber wall. The predicted variation in radial exposure is 5.4% rms with a peak to valley over 30%. This large variation demonstrates the significance of this effect on scattered light, and measurements must account for the effect of the DPR offsets to accurately infer laser absorption during implosions on OMEGA.

The calculated radially integrated total absorbed laser energy over the target [Fig. 4(b)] shows a predicted variation in absorption of 0.84% rms with a peak to valley of 4.8%. By itself, the DPR + CBET-induced nonuniformity was nearly at the 1% rms limit required for successful implosions. When the measured beam energy imbalance (2.2% rms) and mispointing (mean mispointing 19.2 μm,
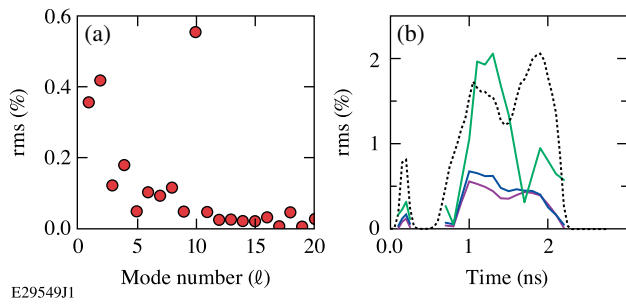
FIG. 5.   (a) The Legendre mode spectrum of the time-integrated absorption and (b) time history of modes 1 (magenta), 2 (blue), and 10 (green) and the normalized laser pulse shape (dotted line).

± 10.4 μm rms) for the implosion were included in the modeling, the total time-integrated rms was predicted to be over 2% with a peak to valley of nearly 13%. The predicted distribution patterns are different for absorption and scattered light, because the former is dominated by the innermost portion of the far-field beam profiles, while the latter is highest for a ring in the outer portion of the profile.

Figure 5(a) shows the Legendre mode decomposition of the time-integrated absorption distribution from Fig. 4(b). The largest mode is $\ell = 10$, which is a result of OMEGA's beam pattern [19]. Otherwise, the spectrum is dominated by the lower modes, primarily $\ell = 1$ and 2. Figure 5(b) shows the laser drive and the time history of the capsule absorption modes. Note that the time-varying mode 10 rms is larger than the time-averaged mode 10, because, as the coronal plasma evolves and the target begins to compress, the beam-induced pattern varies in time, partially averaging itself out. While the modes are relatively small during the laser picket, they are high during the drive portion of the laser pulse when CBET is strongest. The fact that the DPR separation introduces both low- and midmode drive asymmetries is consistent with recent analysis, suggesting both types of nonuniformity are needed to explain experimental observations pertaining to the resultant asymmetry of the implosion core [20].

A relatively simple solution to the issue of DPR $+$ CBET-induced nonuniformity is to fabricate and deploy new DPRs with a decreased spot separation in the far field. Figures 4(c) and 4(d) show the predicted total time-integrated nonuniformity in scattered light and absorption, respectively, using these reduced DPR offset beam intensity profiles. Both the scattered light and the absorption distribution uniformity are predicted to be significantly improved. The absorption rms was reduced to 0.44%, well below the 1% threshold discussed earlier. The scattered-light distribution was reduced by factor of more than 5 to an rms variation of only 0.92%. These new DPRs with a spot separation of 10 μm would greatly reduce the linearly polarized regions where enhanced CBET occurs and concentrate the region to the fringe of the beam where intensities are low. DPRs with a 10-μm spot

separation would still be sufficient to reduce the high-mode, on-target nonuniformity from laser speckles. Fabricating and deploying new 10-μm offset DPRs are presently under review at the Omega Laser Facility and might be implemented as soon as within a year.

In summary, a novel issue for direct-drive implosion uniformity was presented, which was discovered by measuring the uniformity of the scattered light from direct-drive experiments on OMEGA. The implementation of polarization smoothing introduces regions of linear polarization at the edges of the laser spots, which result in nonuniform CBET coupling between beams. Three-dimensional simulations show that this effects leads to a significant nonuniformity in absorbed energy (5.4% peak to valley), which is likely to degrade the implosion performance. A solution to ameliorate the nonuniformity by replacing the polarization smoothing optics is suggested.

[1] J. Nuckolls, L. Wood, A. Thiessen, and G. Zimmerman, Nature (London) 239, 139 (1972).
[2] S. E. Bodner, D. G. Colombant, J. H. Gardner, R. H. Lehmberg, S. P. Obenschain, L. Phillips, A. J. Schmitt, J. D. Sethian, R. L. McCrory, W. Seka et al., Phys. Plasmas 5, 1901 (1998).
[3] V. N. Goncharov, S. P. Regan, E. M. Campbell, T. C. Sangster, P. B. Radha, J. F. Myatt, D. H. Froula, R. Betti, T. R. Boehly, J. A. Delettrez et al., Plasma Phys. Controlled Fusion 59, 014008 (2017).
[4] S. Skupsky and K. Lee, J. Appl. Phys. 54, 3662 (1983).
[5] W. L. Kruer, S. C. Wilks, B. B. Afeyan, and R. K. Kirkwood, Phys. Plasmas 3, 382 (1996).
[6] C. J. Randall, J. J. Thomson, and K. G. Estabrook, Phys. Rev. Lett. 43, 924 (1979).
[7] D. H. Froula, I. V. Igumenshchev, D. T. Michel, D. H. Edgell, R. Follett, V. Yu. Glebov, V. N. Goncharov, J. Kwiatkowski,

F. J. Marshall, P. B. Radha *et al.*, Phys. Rev. Lett. **108,** 125003 (2012).

[8] P. Michel, W. Rozmus, E. A. Williams, L. Divol, R. L. Berger, S. H. Glenzer, and D. A. Callahan, Phys. Plasmas **20,** 056308 (2013).

[9] P. Michel, L. Divol, D. Turnbull, and J. D. Moody, Phys. Rev. Lett. **113,** 205001 (2014).

[10] D. H. Edgell, R. K. Follett, I. V. Igumenshchev, J. F. Myatt, J. G. Shaw, and D. H. Froula, Phys. Plasmas **24,** 062706 (2017).

[11] J. Delettrez, R. Epstein, M. C. Richardson, P. A. Jaanimagi, and B. L. Henke, Phys. Rev. A **36,** 3926 (1987).

[12] T. R. Boehly, D. L. Brown, R. S. Craxton, R. L. Keck, J. P. Knauer, J. H. Kelly, T. J. Kessler, S. A. Kumpan, S. J. Loucks, S. A. Letzring *et al.*, Opt. Commun. **133,** 495 (1997).

[13] See Supplemental Material at http://link.aps.org/supplemental/10.1103/PhysRevLett.127.075001 for further details on the implosion experiments, data analysis, and simulations used in this Letter.

[14] T. R. Boehly, V. A. Smalyuk, D. D. Meyerhofer, J. P. Knauer, D. K. Bradley, R. S. Craxton, M. J. Guardalben, S. Skupsky, and T. J. Kessler, J. Appl. Phys. **85,** 3444 (1999).

[15] D. H. Edgell, J. Katz, D. P. Turnbull, and D. H. Froula, Rev. Sci. Instrum. **89,** 10E101 (2018).

[16] D. H. Edgell, A. M. Hansen, J. Katz, D. Turnbull, and D. H. Froula, Rev. Sci. Instrum. **92,** 043525 (2021).

[17] D. Cao, G. Moses, and J. Delettrez, Phys. Plasmas **22,** 082308 (2015).

[18] I. V. Igumenshchev, D. H. Edgell, V. N. Goncharov, J. A. Delettrez, A. V. Maximov, J. F. Myatt, W. Seka, A. Shvydky, S. Skupsky, and C. Stoeckl, Phys. Plasmas **17,** 122708 (2010).

[19] I. V. Igumenshchev, V. N. Goncharov, F. J. Marshall, J. P. Knauer, E. M. Campbell, C. J. Forrest, D. H. Froula, V. Yu. Glebov, R. L. McCrory, S. P. Regan *et al.*, Phys. Plasmas **23,** 052702 (2016).

[20] A. Bose, R. Betti, D. Mangino, K. M. Woo, D. Patel, A. R. Christopherson, V. Gopalaswamy, O. M. Mannion, S. P. Regan, V. N. Goncharov *et al.*, Phys. Plasmas **25,** 062701 (2018).